Midbody and primary cilium of neural progenitors release extracellular membrane particles enriched in the stem cell marker prominin-1

Véronique Dubreuil,[1] Anne-Marie Marzesco,[1] Denis Corbeil,[2] Wieland B. Huttner,[1] and Michaela Wilsch-Bräuninger[1]

[1]Max Planck Institute of Molecular Cell Biology and Genetics, D-01307 Dresden, Germany
[2]Tissue Engineering Laboratories, Biotec, D-01307 Dresden, Germany

Expansion of the neocortex requires symmetric divisions of neuroepithelial cells, the primary progenitor cells of the developing mammalian central nervous system. Symmetrically dividing neuroepithelial cells are known to form a midbody at their apical (rather than lateral) surface. We show that apical midbodies of neuroepithelial cells concentrate prominin-1 (CD133), a somatic stem cell marker and defining constituent of a specific plasma membrane microdomain. Moreover, these apical midbodies are released, as a whole or in part, into the extracellular space, yielding the prominin-1–enriched membrane particles found in the neural tube fluid. The primary cilium of neuroepithelial cells also concentrates prominin-1 and appears to be a second source of the prominin-1–bearing extracellular membrane particles. Our data reveal novel origins of extracellular membrane traffic that enable neural stem and progenitor cells to avoid the asymmetric inheritance of the midbody observed for other cells and, by releasing a stem cell membrane microdomain, to potentially influence the balance of their proliferation versus differentiation.

Introduction

The midbody is a transient structure formed during the final stage of cell division (Glotzer, 2001; Otegui et al., 2005). Its main cytoplasmic components are the constricted actomyosin-based contractile ring and microtubule bundles derived from the central spindle (Mullins and McIntosh, 1982; Glotzer, 2001). Often in association with these two scaffolds, numerous proteins involved in cytoskeletal organization, cytokinesis, cell cycle regulation, and signaling are concentrated at the midbody (Glotzer, 2001; Schweitzer and D'Souza-Schorey, 2004; Skop et al., 2004; Otegui et al., 2005). Two principal membrane structures exist at the midbody—the plasma membrane, which corresponds to that of the cleavage furrow, and cytoplasmic membrane vesicles of biosynthetic and endocytic origin, which fuse with the plasma membrane for abscission, the terminal step of cytokinesis (Glotzer, 2001; Low et al., 2003; Schweitzer and D'Souza-Schorey, 2004; Gromley et al., 2005; Matheson et al., 2005; Otegui et al., 2005). Beyond abscission, little is known about membrane traffic events involving the midbody.

As for the midbody, microtubule bundles are key cytoskeletal elements of primary cilia (Pazour and Witman, 2003; Snell et al., 2004; Praetorius and Spring, 2005). However, in contrast to the midbody, which forms during M phase, primary cilia are plasma membrane protrusions of interphase and postmitotic cells (Pazour and Witman, 2003; Quarmby and Parker, 2005). Primary cilia have emerged as important structures that function like an antenna and have a key role in signaling to the cell interior, including the regulation of cell cycle progression (Snell et al., 2004; Hildebrandt and Otto, 2005; Huangfu and Anderson, 2005; Pan et al., 2005; Quarmby and Parker, 2005; Tanaka et al., 2005; Hirokawa et al., 2006; Scholey and Anderson, 2006). Considerable progress has been made with regard to transport of proteins within the cilium (Rosenbaum and Witman, 2002; Scholey and Anderson, 2006). However, the dynamics of the ciliary plasma membrane, specifically in the context of the disappearance of the primary cilium before, and its reformation after, M phase, have not been resolved.

Neuroepithelial (NE) cells are the primary progenitor cells of the mammalian central nervous system. They are polarized along their apical–basal axis, and the orientation of the

Correspondence to Wieland B. Huttner: huttner@mpi-cbg.de

V. Dubreuil's present address is UMR 8542, Centre National de la Recherche Scientifique, Ecole Normale Supèrieure, F-75005 Paris, France.

Abbreviations used in this paper: DIC, differential interference contrast; E, embryonic day; HH, Hamburger and Hamilton; mRFP, monomeric red fluorescent protein; NE, neuroepithelial.

The online version of this article contains supplemental material.

The Journal of Cell Biology, Vol. 176, No. 4, February 12, 2007 483–495
http://www.jcb.org/cgi/doi/10.1083/jcb.200608137

cleavage plane relative to this axis determines whether division is symmetric or asymmetric (Götz and Huttner, 2005). NE cells initially increase in number by symmetric divisions, in which cleavage occurs precisely along their apical–basal axis, bisecting the apical plasma membrane domain (hereafter referred to as the apical membrane) of the dividing cell and thus distributing it equally to both daughters (Chenn and McConnell, 1995; Kosodo et al., 2004; Götz and Huttner, 2005). At the onset of neurogenesis, NE cells switch to asymmetric divisions, in which the orientation of the cleavage plane deviates from the apical–basal axis, resulting in the apical membrane being bypassed by the cleavage furrow and hence being inherited by only one of the daughter cells, which thus remains neuroepithelial, in contrast to its sister, which adopts a neuronal fate (Kosodo et al., 2004; Götz and Huttner, 2005). Concomitant with this switch, NE cells reduce the size of their apical membrane (Kosodo et al., 2004). It is unknown whether this reduction is solely achieved by down-regulation of apical biosynthetic transport (Aaku-Saraste et al., 1997) or involves additional dynamics of the apical membrane.

Extracellular membrane vesicles and their origin in eukaryotic cells have received increasing attention. We recently reported the existence in the lumen of the neural tube of two novel classes of extracellular membrane particles that bear a marker of the apical membrane of NE cells, prominin-1 (prom1; Marzesco et al., 2005), which will be collectively referred to as prom1 particles herein. One class consists of small (50–80 nm) electron-translucent vesicles, referred to as P4 particles. The other class comprises relatively large (0.5–1 μm) electron-dense particles, referred to as P2 particles, on which prom1 often appears to be distributed in a ring-like fashion. Importantly, the P4 particles were found to be distinct from the similar-size exosomes (Marzesco et al., 2005), the internal vesicles of multivesicular bodies that are released into the extracellular space by exocytosis (Stoorvogel et al., 2002; Théry et al., 2002; Février and Raposo, 2004). Likewise, the P2 particles appear to be morphologically distinct from the recently reported 0.3–5-μm nodal vesicular parcels implicated in left–right determination (Tanaka et al., 2005).

Given the presence of apical membrane constituents in the P2 and P4 particles (Marzesco et al., 2005), their release would be a means of reducing the size of the apical membrane of NE cells as these cells switch from symmetric to asymmetric division during brain development (Kosodo et al., 2004). Consistent with this possibility, P2 and P4 particles accumulate in the neural tube fluid before (P2) and during (P4) the onset of neurogenesis, and both types of particles decrease as neurogenesis progresses (Marzesco et al., 2005). It is therefore important to identify the subcellular sites from which P2 and P4 particles originate. Although the origin of P2 particles has been enigmatic, microvilli have been considered the likely source of P4 particles (Marzesco et al., 2005), given that microvilli may give rise to small extracellular membrane vesicles (Hobbs, 1980; Beaudoin and Grondin, 1991) and that the P4 particle constituent prom1 is concentrated on microvilli of NE cells (Weigmann et al., 1997). However, at the onset of neurogenesis, when the P4 particles accumulate in the neural tube fluid, most NE cells bear only few, if any, microvilli (Marzesco et al., 2005), raising the possibility that NE cell structures other than microvilli give rise to P4 particles.

Prom1, the characteristic membrane constituent of the P2 and P4 particles, has intriguing features. First, prom1, also called CD133 (Fargeas et al., 2003), is not only found on NE cells but is widely expressed by many somatic stem cells (Weigmann et al., 1997; Yin et al., 1997; Corbeil et al., 2001; Lee et al., 2005; Fargeas et al., 2006). Second, being a pentaspan membrane protein, prom1 is the defining constituent of a specific, cholesterol-based membrane microdomain that is characteristic of various types of plasmalemmal protrusions exhibiting substantial membrane curvature (Weigmann et al., 1997; Röper et al., 2000; Corbeil et al., 2001). Collectively, these findings imply that the release of the prom1 particles into the neural tube fluid would be a means of not only reducing the size of the apical membrane of NE cells but also modifying its composition by depleting a stem cell–characteristic membrane microdomain. Here, we show that prom1 is concentrated at apical midbodies of symmetrically dividing NE cells and, after the onset of neurogenesis, on primary cilia, and that these NE cell surface structures are the sites of origin of extracellular prom1 particles.

Results

Release of prom1 particles from the apical surface of NE cells

We focused on the neuroepithelium as a source of prom1 particles because the neural tube fluid of the mouse embryo has previously been shown to contain both P2 and P4 membrane particles (Marzesco et al., 2005) and NE cells express prom1 on their lumenal surface (Weigmann et al., 1997). To investigate the formation of the prom1 particles, a mouse prom1-GFP fusion protein was expressed in the embryonic chick spinal cord neuroepithelium, which is structurally very similar to the mouse neuroepithelium, but a simpler experimental system (Krull, 2004). Prom1-GFP was expressed at Hamburger and Hamilton (HH) stage 10–11 and analyzed 24 h later (HH17), i.e., at the onset of neurogenesis. Remarkably, prom1-GFP was not only concentrated at the apical surface of the transfected side of the neuroepithelium (Fig. 1, A, C, and D, open arrow) but also detected as punctate structures at the surface of the contralateral, untransfected side of the neuroepithelium (Fig. 1, C and D, arrowheads). Higher magnification revealed that the punctate structures had a ring-like appearance (Fig. 1, C and D, insets), as previously reported for the P2 particles enriched in prom1 (Marzesco et al., 2005). In contrast to prom1-GFP, monomeric red fluorescent protein (mRFP), which was cotransfected with prom1-GFP, remained confined to the transfected side of the neuroepithelium (Fig. 1, B and D). These observations suggested that the prom1-GFP particles associated with the contralateral neuroepithelium originated from the transfected side by some transfer of membrane.

To explore this possibility, prom1-GFP was expressed in the chick spinal cord (HH10–11), and slice cultures prepared 24 h later were analyzed by time-lapse confocal imaging. This revealed the presence of pleiomorphic prom1-GFP particles in

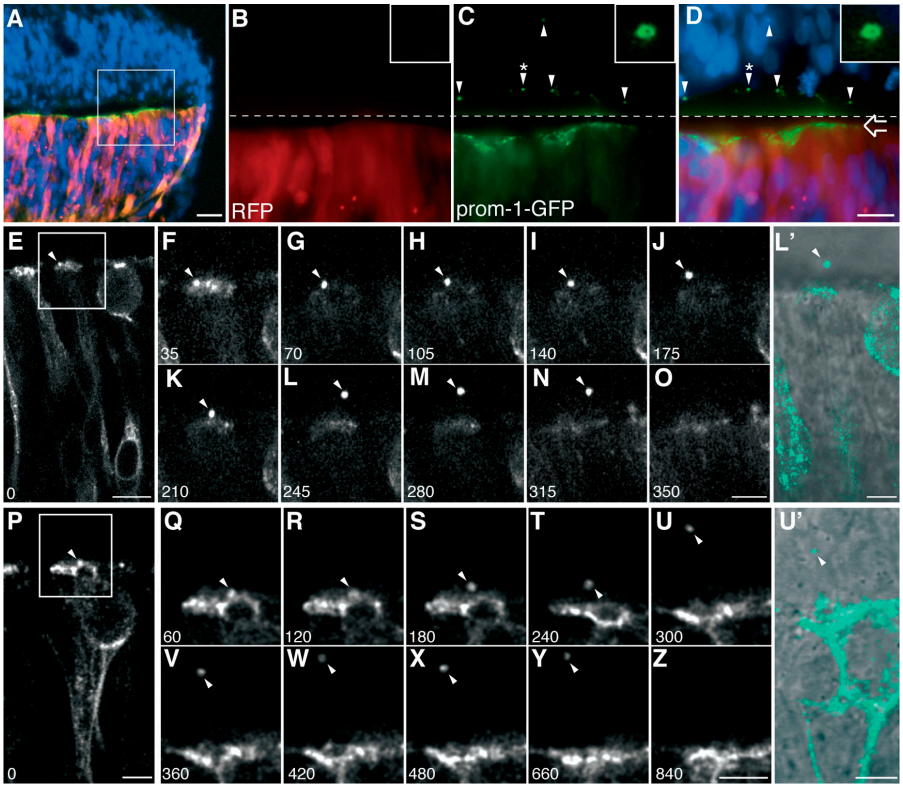

Figure 1. **Release of prom1-GFP–bearing particles from the apical surface of NE cells.** Chick spinal cord (HH10–11) was coelectroporated with prom1-GFP and mRFP and analyzed 24 h later. (A–D) Transverse cryosection of fixed spinal cord analyzed by conventional fluorescence microscopy. DAPI is in blue, mRFP is in red, and prom1-GFP is in green. (A) Low-magnification overview. (B–D) Higher magnification of mRFP (B) and prom1-GFP (C) fluorescence in the area indicated by the white square in A; the merge in D includes the DAPI staining of nuclei. The top half of the images (i.e., above the dashed line) has been contrast enhanced for mRFP and prom1-GFP to facilitate detection of the prom1-GFP–bearing particles at the apical surface of, and within, the nontransfected, contralateral side of the neuroepithelium (arrowheads). The open arrow indicates the apical surface of transfected side of the neuroepithelium. The insets show a higher magnification of the prom1-GFP–bearing particle indicated by the arrowheads with asterisks. (E–Z) Slice cultures were subjected to time-lapse confocal imaging of prom1-GFP, using either 35-s (E–O) or 60-s (P–Z) intervals. The time points shown are indicated in the bottom left corner of each panel (in seconds). Selected single optical sections, following the prom1-GFP–bearing particle (arrowheads) through the z stack, are shown. The apical surface of the transfected side of the neuroepithelium is up. In E, note the basal position of the nucleus of the NE cell releasing the prom1-GFP–bearing particle. (F–O and Q–Z) Higher magnification of the area indicated by the white rectangle in E and P, respectively. (L' and U') Overlay of the DIC image and the prom1-GFP fluorescence (green) corresponding to L and U, respectively; note the localization of the prom1-GFP–bearing particle in the lumen of the neural tube (L') and in the contralateral neuroepithelium (U'). Bars: (A) 20 μm; (D and E) 10 μm; (P, O, Z, L', and U') 5 μm.

the lumen of the neural tube that rapidly passed through the field of observation (Video 1, available at http://www.jcb.org/cgi/content/full/jcb.200608137/DC1). Despite the dynamic movement of these particles, their generation from the apical surface of the transfected NE cells could be captured in some cases with the present experimental setup (Fig. 1, E–Z). In these instances, prom1-GFP appeared to concentrate within the apical membrane, followed by release of a particle from the surface of the transfected NE cell (Fig. 1, E–N and P–Y; and Videos 1 and 2). After its release, the prom1-GFP particle quickly disappeared from the imaged field (Fig. 1, O and Z; and Videos 1 and 2). Interestingly, a released particle appeared to be able to enter the contralateral neuroepithelium (Fig. 1, U–Y and U'). We conclude that prom1 particles are released from the apical surface of NE cells into the neural tube lumen.

The midbody as a candidate donor membrane for prom1 particles

To identify the sites of origin of the prom1 particles, we explored the possibility that these particles may originate from microtubule-based plasma membrane protrusions. The rationale for this was that prom1 is known to be concentrated in plasma membrane protrusions (Weigmann et al., 1997; Corbeil et al., 2001), but the majority of the prom1 particles in the neural tube fluid lack actin (Marzesco et al., 2005). Indeed, upon differential centrifugation of embryonic day (E) 11.5 mouse neural tube fluid followed by immunoblotting, the P2 pellet, in which most of the large prom1 particles are known to be recovered (Marzesco et al., 2005), showed a striking enrichment of α-tubulin (Fig. 2 A). Consistent with this, double immunofluorescence of the prom1 particles in the lumen of the telencephalic ventricles revealed that a substantial fraction of them (57 ± 11%) contained α-tubulin, which appeared to be concentrated in the center of the ring-like prom1 staining (Fig. 2 B). Double immunogold EM of the P2 pellet corroborated this conclusion (Fig. 2 E) and revealed, for the E10.5 telencephalon, α-tubulin inside electron-dense structures that showed prom1 labeling at their surface and that appeared to be detached (or at least emerging) from the apical surface of the neuroepithelium (Fig. 2, C and D).

In light of these observations, we considered as putative donor membranes for the lumenal prom1 particles two apical membrane structures of NE cells that are known to be associated with clusters of microtubules, the cilium (Pazour and Witman, 2003; Praetorius and Spring, 2005) and the midbody, a cytoplasmic bridge connecting nascent daughter cells until the completion of cytokinesis (Glotzer, 2001; Otegui et al., 2005). EM of serial plastic sections of apical midbodies of dividing NE cells in the mouse E10.5 telencephalon yielded three principal results. First, we observed membrane buds of various sizes emerging from midbodies, as well as vesicular profiles in their immediate vicinity (Fig. 3, A, D, and E, arrowheads; and Fig. S4, A and B, available at http://www.jcb.org/cgi/content/full/jcb.200608137/DC1), consistent with extracellular membrane vesicles arising from midbodies.

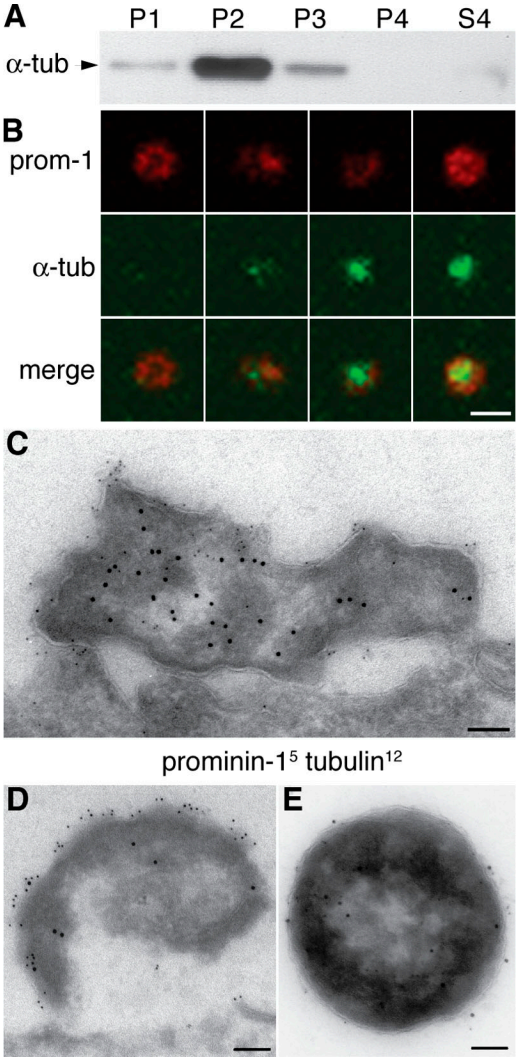

Figure 2. **Prom1 particles contain α-tubulin.** (A) Neural tube fluid of E11.5 mouse embryos was subjected to differential centrifugation (Marzesco et al., 2005) followed by immunoblot analysis of the fractions for α-tubulin. P1, 300-*g* pellet; P2, 1,200-*g* pellet; P3, 10,000-*g* pellet; P4, 100,000-*g* pellet; S4, 100,000-*g* supernatant. (B) Transverse cryosection of E10.5 mouse telencephalon double immunostained for prom1 (red) and α-tubulin (green) and analyzed by confocal microscopy; four examples of prom1 particles in the lumen of the telencephalic ventricle are shown (z-stack projection). (C and D) Transverse ultrathin cryosections of the apical region of mouse E10.5 telencephalic NE cells immunogold labeled for prom1 (5 nm) and α-tubulin (12 nm) showing two doubly immunoreactive particles at the lumenal surface. (E) Negative staining of a particle from the P2 pellet after immunogold labeling for prom1 (5 nm) and acetylated tubulin (12 nm). Bars: (B) 1 μm; (C–E) 100 nm.

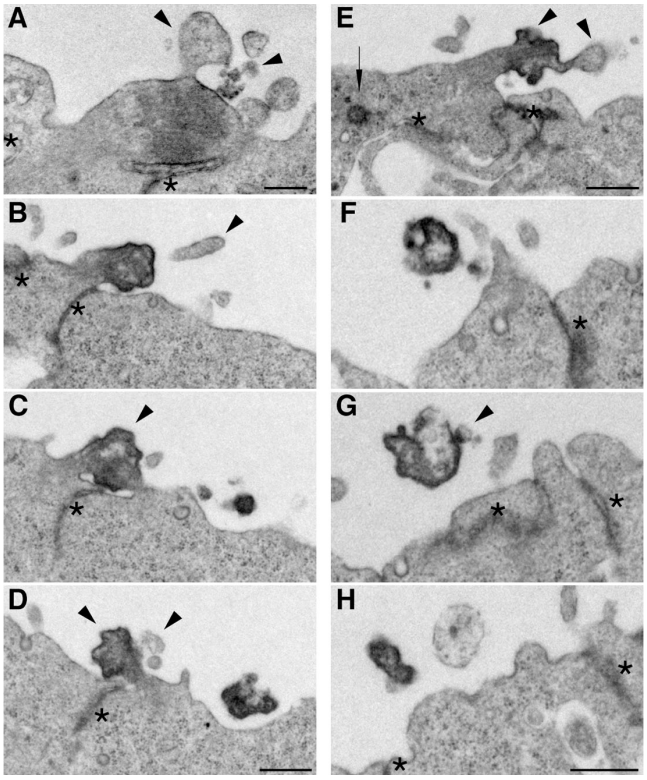

Figure 3. **Ultrastructural resemblance of lumenal particles to aged midbodies of NE cells.** EM analysis of serial ultrathin (70 nm) plastic sections of the apical surface of E10.5 mouse telencephalic neuroepithelium. (A) Midbody connecting NE daughter cells in telophase. (B–D) Series showing every other section of an aged midbody. (E) Midbody of an NE cell that has relocated the centriole (arrow) apically. (F–H) Series showing every third section of an electron-dense particle detached from the apical surface of the neuroepithelium. Arrowheads indicate plasma membrane buds and protrusions, and asterisks indicate adherens junctions. The complete sequence of serial sections from which A, E, and F–H were selected is shown in Fig. S4 (A–C), respectively (available at http://www.jcb.org/cgi/content/full/jcb.200608137/DC1). Bars, 500 nm.

Second, although certain midbodies showed the typical ordered array of microtubules and could be identified as such in single sections (Fig. 3 A), others showed the same morphological appearance as the previously observed pleiomorphic protuberances (Marzesco et al., 2005) and could only be identified as a midbody upon serial sectioning (Fig. 3, B–E; and Fig. S4 B). In the case of the latter midbodies, an ordered array of microtubules was less obvious (Fig. 3, C and E), and the texture of the cytoplasm in the core region appeared more heterogeneous, showing more electron-dense areas (usually in the cortical region) as well as less condensed patches (Fig. 3, C and E). Moreover, these midbodies were usually observed on NE daughter cells that appeared to have entered G1 by morphological criteria, such as (1) the presence of a cilium, which is known to be disassembled during M phase (Hinds and Ruffett, 1971; Cohen et al., 1988; Pazour and Witman, 2003; Quarmby and Parker, 2005) and to reform thereafter (Fig. S4 B), (2) an elongated cell shape (Fig. 1, E and P; and not depicted), and (3) an abventricular position of the nucleus (Fig. 1, E and P; Fig. S4 A; Hinds and Ruffett, 1971). Given this temporal relationship, we will refer to these as "aged" midbodies.

Third, we observed pleiomorphic membrane structures that, as revealed by serial sectioning, were clearly detached from the apical surface of NE cells, but whose morphology was otherwise similar to that of the core of aged midbodies (Fig. 3, F–H). As these detached membrane structures were reminiscent in appearance of the P2 particles in the neural tube lumen (Fig. 2, C and D; Fig. S2, available at http://www.jcb.org/cgi/content/full/jcb.200608137/DC1; Marzesco et al., 2005), our observations collectively suggest that the latter particles may originate from the midbody.

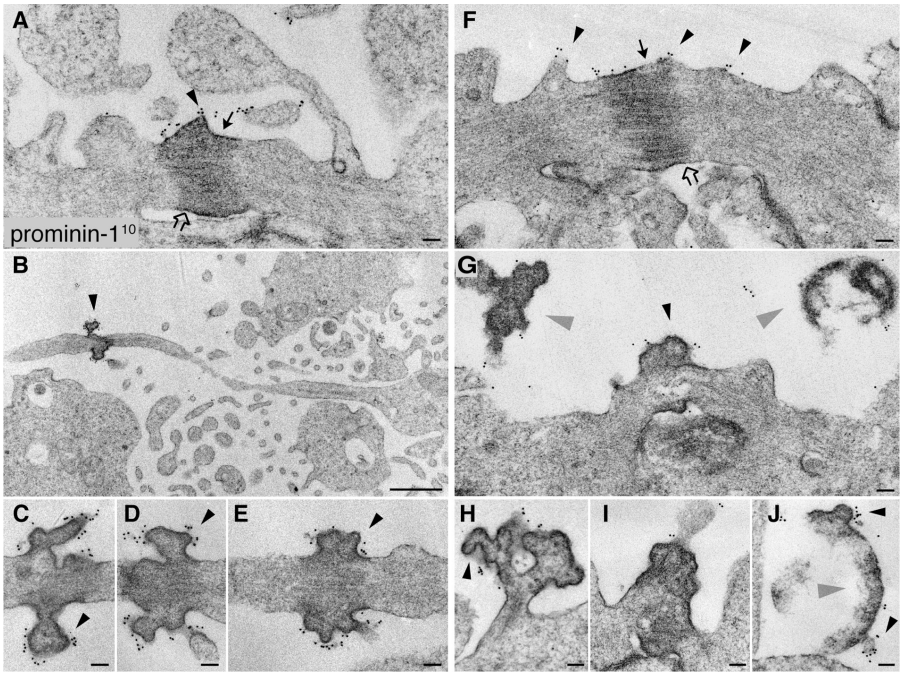

Figure 4. **Prom1 is concentrated at the midbody of NE cells.** Mouse embryonic forebrain was subjected to preembedding immunogold labeling for prom1 (10 nm gold) followed by EM analysis of ultrathin serial plastic sections. Apical midbodies of NE cells at E8.5 (A–E), E10.5 (H–J), and E12.5 (F and G) are shown. (B and C) The central portion of the midbody with long, thin stalks depicted in B is shown at higher magnification of a consecutive section in C. (D and E) Consecutive sections showing the central portion of another midbody with long, thin stalks. (G–I) Midbodies with short stalks. (J) Particle at the apical surface of a neuroepithelial cell. Black arrowheads indicate prom1-labeled plasma membrane buds and protrusions, gray arrowheads indicate detached particles, solid arrows indicate midbody plasma membrane facing the lumenal side, and open arrows indicate midbody plasma membrane derived from cleavage furrow. Bars: (A and C–J) 100 nm; (B) 1 μm.

Prom1 is concentrated at the midbody of NE cells

If P2 particles originate from the midbody, one would expect prom1 to be concentrated there. Immunogold labeling EM showed that this was indeed the case. Specifically, prom1 was clustered at the surface of the electron-dense central portion of the midbody (Fig. 4, A and F). Remarkably, prom1 labeling was particularly strong at buds emerging from the central midbody plasma membrane (Fig. 4, C, D, and G, arrowheads).

Comparison of various embryonic stages revealed that midbodies in which the electron-dense central region was connected to the daughter cells via relatively short stalks were observed both before (E8.5; Fig. 4 A) and after (E12; Fig. 4, F, G, and I) the onset of neurogenesis in the telencephalon, whereas midbodies with long, thin stalks (Fig. 4 B) were only detected at an early stage (E8.5). Prom1 immunolabeling of the various midbodies yielded three observations worth noting. First, in the case of short midbodies with an ordered array of microtubules, prom1 was mostly detected on the plasma membrane domain facing the lumen (Fig. 4, A and F, solid arrows), rather than on the membrane domain derived from the cleavage furrow (open arrows). This is consistent with the former midbody plasma membrane domain corresponding to the prom1-bearing, apical membrane of the mother cell. Second, in the case of aged midbodies, which had short or long stalks, prom1 appeared to surround the central core (Fig. 4, C–E), suggesting that midbody aging is accompanied by membrane microdomain redistribution. Third, in the case of the long, thin midbodies, prom1 was confined to the very central portion (Fig. 4, B and E), indicating that this represented a distinct membrane subdomain.

In addition, the immunogold labeling of the apical surface of the neuroepithelium revealed that small (30–60-nm diameter) membrane buds with clustered prom1 were observed not only on the central portion of the midbody (Fig. 4, C–E and H) but also on relatively large (1-μm diameter) structures detached from, but nonetheless in the vicinity of, the apical surface of NE cells (Fig. 4, G and J, gray arrowheads). This suggests that the small (50–80 nm) P4 prom1 particles in the neural tube fluid (Marzesco et al., 2005) may originate not only from apical membrane protrusions of NE cells such as microvilli (Marzesco et al., 2005; for cilia, see Fig. 7) but also from the larger P2 prom1 particles in the neural tube lumen that in turn have originated from the midbody of NE cells.

Prom1 particles contain anillin, a component of the midbody

A characteristic component of the midbody is anillin, an actin-binding protein associated with the contractile ring (Field and Alberts, 1995; Oegema et al., 2000). If the prom1 particles found in the neural tube fluid arise from the midbody, one might expect them to contain anillin. Indeed, double immunogold labeling of E10.5 telencephalic NE cells revealed that not only apical midbodies contained anillin (in addition to prom1; Fig. 5 A), but also the prom1 particles that had detached from the apical surface (Fig. 5 B) and could be isolated from the neural tube fluid (Fig. 5 C, arrowheads). By double immunofluorescence, a substantial portion (39 ± 8%) of the prom1 particles in the lumen of the E10.5 telencephalic ventricle contained anillin (Fig. 5 F). Furthermore, the vast majority of anillin-positive structures at the apical surface of the E11.5 telencephalic neuroepithelium also contained prom1 (Fig. 5 D, arrowheads), although within each structure, the distribution of the two markers relative to one another was distinct (Fig. 5 E). These findings corroborate our conclusion that prom1 particles in the neural tube fluid arise from the midbody of NE cells.

Given these observations with fixed samples, we performed time-lapse confocal imaging of live dividing NE cells in slice culture after expression of GFP-anillin in the chick spinal

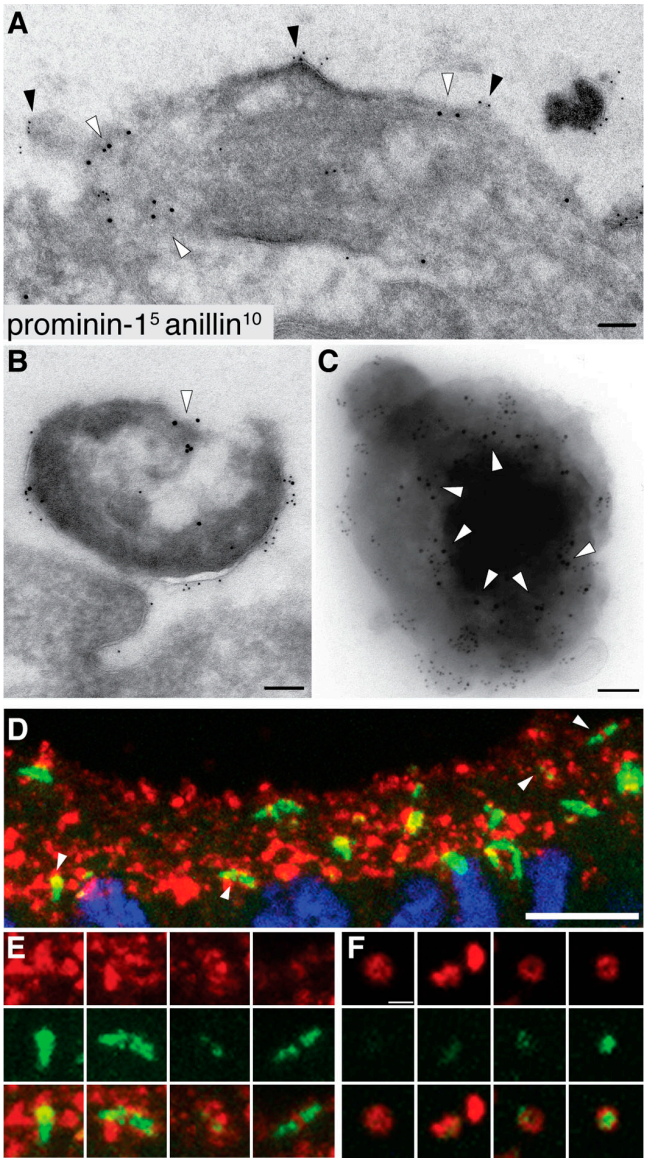

Figure 5. **Anillin is present not only in prom1-bearing midbodies but also in prom1-bearing lumenal particles.** (A and B) Transverse ultrathin cryosections of the apical surface of E10.5 mouse telencephalic neuroepithelium double immunogold labeled for prom1 (5 nm) and anillin (10 nm; white arrowheads). Doubly immunoreactive midbody (A) and particle at the apical surface of the neuroepithelium (B). Black arrowheads indicate prom1-labeled regions at the lumenal plasma membrane of the midbody. (C) Double immunogold labeling for prom1 (5 nm) and anillin (10 nm; white arrowheads) of a particle from the P2 pellet of E11.5 neural tube fluid. (D–F) Transverse cryosections of E11.5 (D and E) and E10.5 (F) mouse telencephalon double immunostained for prom1 (red) and anillin (green) and analyzed by confocal microscopy. (D and E) Z-stack projection providing an en face view onto the apical surface of the neuroepithelium; for orientation, the DAPI staining of nuclei (blue) is shown for one of the optical sections in D. (E) Selected regions of D (indicated by arrowheads) at higher magnification. (F) Four examples of prom1-bearing particles in the lumen of the telencephalic ventricle (z-stack projection). Bars: (A–C) 100 nm; (D) 10 μm; (F) 1 μm.

cord (Fig. S1 and Video 3, available at http://www.jcb.org/cgi/content/full/jcb.200608137/DC1). This revealed that after its release from the nucleoplasm into the cytoplasm upon nuclear envelope breakdown, GFP-anillin clustered at the basal pole of the cell body, associated with the contractile ring, and became concentrated in particles that formed at the apical surface of the dividing cell at the end of cytokinesis. These apical GFP-anillin–containing particles eventually disappeared from the daughter cells, consistent with them being released into the neural tube lumen.

Apical midbodies and symmetric versus asymmetric divisions of NE cells

It has previously been reported that, depending on whether an NE cell undergoes symmetric or asymmetric division, the cleavage furrow ingressing from the basal side will either bisect or bypass the apical membrane, resulting in its inheritance by both or only one of the daughter cells, respectively (Kosodo et al., 2004). A corollary of this is that in a symmetric division, the midbody contains apical membrane, whereas in an asymmetric division, it does not. In light of the present findings, we extended previous observations related to this issue (Kosodo et al., 2004) and systematically determined the localization of midbodies relative to the apical, prom1-containing membrane of telophase NE cells. This analysis was performed in *Tis21*-GFP knockin mouse embryos, in which GFP is specifically expressed in NE cells undergoing neurogenic (rather than proliferative) divisions (Haubensak et al., 2004); neurogenic (*Tis21*-GFP–positive) divisions at the ventricular surface are predominantly (but not exclusively) asymmetric, whereas proliferative (*Tis21*-GFP–negative) divisions are nearly always symmetric (Kosodo et al., 2004).

Our first approach was double-immunofluorescence analysis for anillin versus prom1 localization in E11.5 forebrain NE cells in telophase. Fig. 6 (A–E) shows an example of the frequently observed cases of an anillin-labeled midbody being colocalized with prom1, which is consistent with the results of Figs. 4 and 5; the corresponding NE cell lacked *Tis21*-GFP expression (Fig. 6 A) and, hence, most probably underwent a proliferative division. Fig. 6 (F–J), in contrast, shows an example of the fewer cases of an anillin-labeled midbody being located just underneath the ventricular surface and lacking prom1; here, the corresponding NE cell showed *Tis21*-GFP expression (Fig. 6 F), i.e., underwent a neurogenic division. These data on anillin versus prom1 localization were corroborated by 3D reconstruction (Fig. 6, E′ and J′).

Further support for the notion that the release of midbodies containing apical, prom1-enriched membrane is characteristic of NE cells undergoing symmetric, proliferative division was obtained when we identified the apical membrane of single mitotic NE cells by counterstaining for the lateral membrane protein cadherin (Kosodo et al., 2004). Specifically, we determined by double-immunofluorescence analysis of E11.5 forebrain NE cells in telophase whether an anillin-labeled midbody was colocalized with the cadherin "hole" (Kosodo et al., 2004), i.e., the apical membrane, or with the lateral membrane including the cadherin-stained adherens junction. Fig. 6 (K–O) and the 3D reconstruction (Fig. 6 O') show an example of an anillin-labeled midbody being colocalized with the cadherin hole (apical midbody); together with the lack of *Tis21*-GFP expression (Fig. 6 K), this indicated that the corresponding NE cell underwent a symmetric, proliferative division. In contrast, Fig. 6 (P–T)

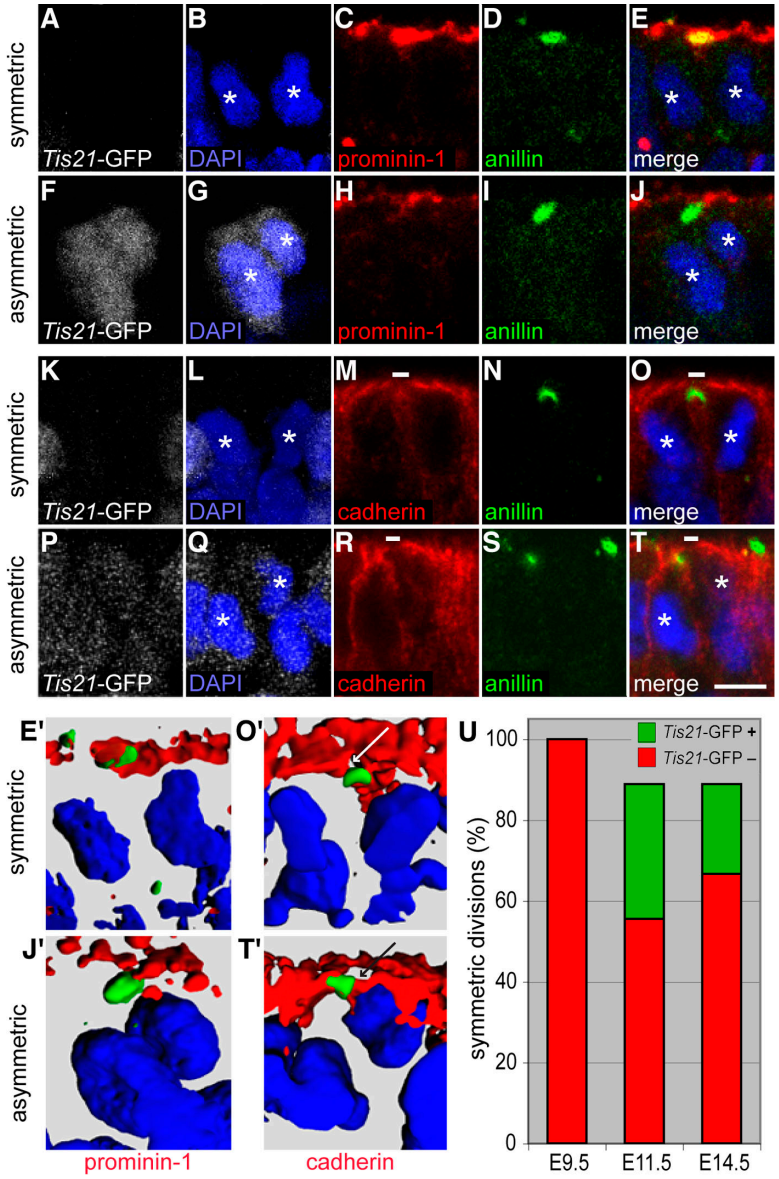

Figure 6. **Localization of anillin relative to prom1 and cadherin in *Tis21*-GFP–negative versus –positive mitotic NE cells.** (A–T) Transverse cryosections of E11.5 forebrain of *Tis21*-GFP knockin mice (GFP expression; white) double immunostained for anillin (green) and either prom1 (A–J; red) or cadherin (K–T; red) and analyzed by confocal microscopy (C–E, H–J, M–O, and R–T, single optical sections; A, B, F, G, K, L, P, and Q, projection of four consecutive optical sections). Nuclei are stained by DAPI (blue). White asterisks indicate telophase nuclei of daughter cells. Small white bars in M, O, R, and T indicate cadherin hole. (A–E and K–O) Telophase NE cells lacking *Tis21*-GFP expression and undergoing symmetric division (anillin colocalized with prom1 and cadherin hole upon 90–100% complete ingression of the cleavage furrow). (F–J and P–T) Telophase NE cells showing strong (F) or weak (P) *Tis21*-GFP expression and undergoing asymmetric division (anillin distinct from prom1 and colocalized with cadherin upon 90–100% complete ingression of the cleavage furrow). (E′, J′, O′, and T′) 3D reconstruction from six to eight 1-μm optical sections showing the prom1–anillin–DAPI merge of the symmetrically dividing *Tis21*-GFP–negative cell in E (E′), the asymmetrically dividing *Tis21*-GFP–positive cell in J (J′), the cadherin–anillin–DAPI merge of the symmetrically dividing *Tis21*-GFP–negative cell in O (O′), and the asymmetrically dividing *Tis21*-GFP–positive cell in T (T′). White and black arrows in O′ and T′, respectively, indicate the cadherin hole. (U) Quantitation of anillin-stained apical midbodies in symmetrically versus asymmetrically dividing NE cells. Forebrain NE cells of E9.5, E11.5, and E14.5 *Tis21*-GFP knockin mice were double immunostained for cadherin and anillin and analyzed by confocal microscopy as in K–T. Telophase NE cells showing 90–100% complete ingression of the cleavage furrow (25 out of 54 cells analyzed) were first scored for colocalization of the apical anillin staining with either cadherin-negative (symmetric division) or cadherin-positive (asymmetric division) segments of the cell surface and then for the absence or presence of *Tis21*-GFP expression. Symmetrically dividing NE cells are expressed as a percentage of symmetrically dividing plus asymmetrically dividing cells; the percentage of symmetrically dividing *Tis21*-GFP–positive cells is indicated in green. Bar, 5 μm.

and the 3D reconstruction (Fig. 6 T′) show an example of an anillin-labeled midbody being colocalized with the cadherin-stained adherens junction (subapical midbody); together with the presence of (albeit weak) *Tis21*-GFP expression (Fig. 6 P), this indicated that the corresponding NE cell underwent an asymmetric, neurogenic division.

We quantified the localization of the midbody relative to the apical versus lateral membrane of telophase NE cells in the forebrain at three developmental stages (Fig. 6 U). After the onset of neurogenesis (E11.5) through midneurogenesis (E14.5), ∼90% of NE cell divisions at the ventricular surface were symmetric and ∼10% asymmetric. (Consistent with previous observations [Kosodo et al., 2004], some of these symmetric divisions were *Tis21*-GFP positive [Fig. 6 U, green].) In contrast, before the onset of neurogenesis (E9.5), essentially all anillin-labeled midbodies were localized to the cadherin hole and none of the NE cells yet expressed *Tis21*-GFP, consistent with the notion that at this stage all NE cells undergo symmetric, proliferative divisions and the midbodies released from these cells contain apical membrane, accounting for the accumulation of the P2 prom1 particles in the neural tube fluid before neurogenesis (Marzesco et al., 2005).

Prom1 appears on cilia of NE cells with neurogenesis

Besides the midbody, cilia are microtubule-based protrusions of the plasma membrane (Pazour and Witman, 2003; Praetorius and Spring, 2005). Given that NE cells are known to bear a primary cilium on their apical surface (Hinds and Ruffett, 1971; Cohen et al., 1988), and the presence of α-tubulin in the P2-type prom1 particles in the lumen of the neural tube (Fig. 2), we investigated whether prom1 is associated with the cilia of NE cells. Transmission EM analysis of mouse forebrain neuroepithelium subjected to preembedding immunogold labeling for prom1 showed that at E8.5, i.e., before the onset of neurogenesis, most (if not all) cilia lacked prom1 (Fig. 7 A). In contrast, at

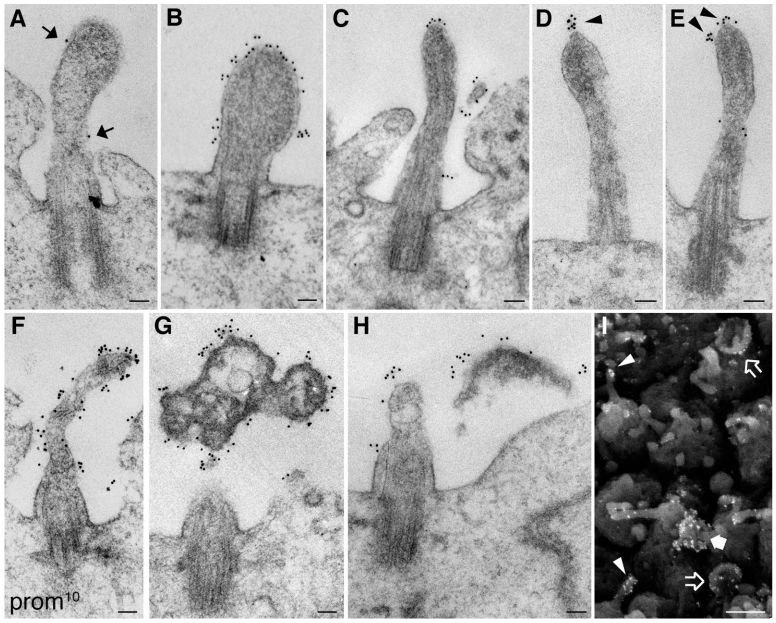

Figure 7. **Prom1 is concentrated on cilia of NE cells.** Mouse forebrain was subjected to preembedding immunogold labeling for prom1 (10 nm gold) followed by EM analysis of ultrathin plastic sections. (A) A cilium at E8.5 showing weak labeling (arrows). (B–F) Cilia at E10.5 (B and C), E12.5 (D and F), or E13.5 (E) showing different degrees of surface labeling; note the cluster of prom1 at the tip of the cilium in D and E (arrowheads). (G and H) Short cilia at E12.5 with strongly prom1-labeled electron-dense particles in their immediate vicinity. (I) Scanning EM of prom1-labeled E10.5 telencephalic ventricular surface; gold particles (18 nm) appear as white dots. Gold-labeled cilia (arrowheads), cup-shaped structures (open arrows), and a strongly immunoreactive protrusion (solid arrow) are indicated. Bars: (A–H) 100 nm; (I) 1 μm.

E10.5 (Fig. 7, B and C) and E12.5–13.5 (Fig. 7, D–F and H), i.e., at the onset and during the early stages, respectively, of neurogenesis in the telencephalon, an increasing proportion (>50%) of cilia of NE cells contained prom1 on their surface. The amount and distribution of prom1 was variable, with some cilia being labeled over most of their surface (Fig. 7, B and F) and others being labeled preferentially at their tips (Fig. 7, C–E). In some cases, the clustering of prom1 at the tip of the cilium was suggestive of a membrane budding process (Fig. 7, D and E, arrowheads). In addition, we occasionally observed electron-dense, strongly prom1-immunoreactive particles in the immediate vicinity of cilia that, remarkably, were rather short (Fig. 7, G and H). An overview by scanning EM of the immunogold-labeled ventricular surface of E10.5 forebrain neuroepithelium corroborated the presence of prom1 on cilia (Fig. 7 I, arrowheads) and other apical membrane structures (arrows).

Discussion

Release of apical midbodies of NE cells as P2 prom1 particles

We report a novel role of the midbody and primary cilium, the removal of a stem cell–characteristic membrane microdomain from somatic stem and progenitor cells via the release of extracellular membrane particles. Our study shows that apical midbodies of NE cells are the source of the P2 particles in the neural tube lumen that show a ring-like prom1 immunostaining (Marzesco et al., 2005). The evidence includes (1) the resemblance in overall morphology between the electron-dense particles in the neural tube lumen (Fig. 3, F–H) and the central portion of apical midbodies (Fig. 3, B–E); (2) the enrichment of tubulin, which is known to be particularly concentrated in the central portion of the midbody (Mullins and McIntosh, 1982; Fig. 2 C), in the P2 particles (Fig. 2, A, B, and E); (3) the presence of anillin, a marker of the midbody (Oegema et al., 2000; Fig. 5), in the P2 particles; and (4) the clustering of prom1 at the central portion of the midbody plasma membrane (Fig. 4). In fact, the ring-like appearance of the prom1-stained P2 particles in the neural tube lumen (Marzesco et al., 2005; Fig. 1, C and D; Fig. 2 B; and Fig. 5 F) is strikingly reminiscent of the midbody ring (Gromley et al., 2005). Considering the midbody ring structure and the present observations together, we suggest that the P2 particles in the neural tube lumen showing ring-like prom1 staining reflect the release of the central portion of apical midbodies from NE cells into the ventricular fluid (Fig. 8 B, pathway 1).

The fate of the midbody after completion of cytokinesis, including its possible release, has been discussed in previous EM studies on NE and other cells (Buck and Tidsale, 1962a,b; Robbins and Gonatas, 1964; Allenspach and Roth, 1967; Jones, 1969; Bancroft and Bellairs, 1975; Bellairs and Bancroft, 1975; Mullins and Biesele, 1977; Nagele and Lee, 1979). However, conclusive evidence showing that a midbody is actually detached from both daughter cells, which requires serial sectioning transmission EM, has so far been provided in only one of these studies, in which a human bone marrow–derived cell line was investigated in vitro (Mullins and Biesele, 1977). Previous observations with NE cells have been inconclusive as to whether the midbody fully detaches or remains with one of the daughter cells, and their interpretation by the respective investigators has been contradictory (Allenspach and Roth, 1967; Bancroft and Bellairs, 1975; Bellairs and Bancroft, 1975; Nagele and Lee, 1979). Moreover, although some investigators have assumed that the midbody may be discarded after each cell division (Golsteyn et al., 1994), more recent studies with HeLa cells have supported the widely held view that the midbody is inherited by one of the daughter cells (Mishima et al., 2002; Gromley et al., 2005). The evidence presented in this paper, obtained by serial sectioning EM of neuroepithelium (Fig. 3 and Fig. S4 C); immunoblotting, immunofluorescence, and immuno-EM analyses of isolated neural tube fluid (Figs. 2 and 5); and live imaging of prominin-GFP and GFP-anillin release from NE cells

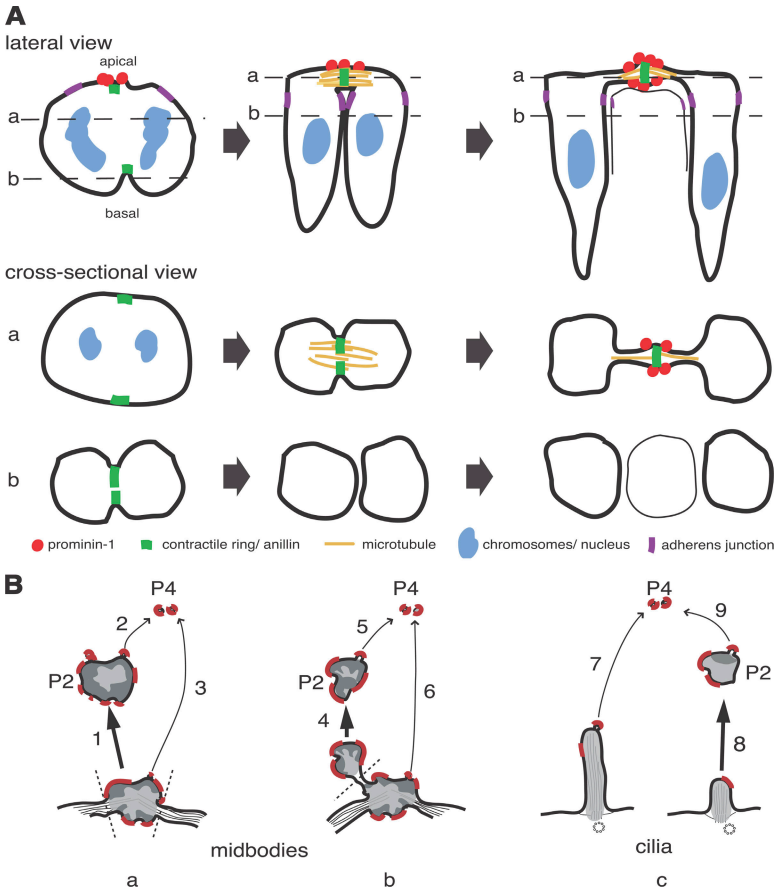

Figure 8. **Depictions of the formation of prom1-bearing extracellular membrane particles from apical midbodies of NE cells.** (A) Three stages (from left to right) of cleavage furrow ingression and apical midbody formation. The top row shows a lateral view, and middle and bottom rows show cross-sectional views at the levels indicated by the dashed lines in the top row. Red indicates prom1, yellow indicates midzone microtubules, green indicates contractile ring/anillin, purple indicates adherens junctions, and blue indicates chromosomes/nuclei. (B) Model showing possible pathways of formation of the P2 prom1 particles (thick arrows; 1, 4, and 8) and P4 particles (thin arrows; 2, 3, 5, 6, 7, and 9) from the apical midbody (a and b) and the primary cilium (c) of NE cells. Dashed lines indicate sites of membrane fission. P2 particles arising by pathway 1 (a) would consist of the entire midbody, explaining the presence of tubulin and anillin in these particles (see Figs. 2 and 5), whereas those arising by pathway 4 (b) and pathway 8 (c) would consist only of parts of the midbody and the cilium, respectively, explaining the existence of P2 particles lacking tubulin and anillin (see Fig. 2 B and Fig. 5 F). Red indicates prom1-containing membrane microdomain.

(Fig. 1 and Videos 1–3), demonstrates that apical midbodies are released from NE cells into the extracellular space.

Such a release implies two sets of membrane fusion events, one on either side of the midbody ring (Fig. 8 B, a, dashed lines). The first fusion constitutes abscission, which terminates cytokinesis (Gromley et al., 2005) and, hence, the connection between the NE daughter cells. The second fusion then releases the central portion of the midbody containing the midbody ring as a P2 prom1 particle from one of the NE daughter cells into the neural tube fluid. At present, very little is known about the molecular machinery mediating midbody release, as compared with the abscission step in HeLa cells (Low et al., 2003; Gromley et al., 2005). (Prom1, used in the present study as a marker to monitor the release of the midbody, does not appear to be essential for this release. Comparison of wild-type and prom1 knockout mice did not reveal an obvious difference in the number of P2 particles in the neural tube, using either immunofluorescence for the midbody protein CRIK [citron rho interacting kinase] or conventional EM [unpublished data].) However, time-lapse imaging of the release of prom1-GFP–labeled and GFP-anillin–labeled particles from NE cells provided clues as to when during the cell cycle this release takes place. We observed that the release of prom1- and anillin-bearing P2 particles occurred from NE cells whose nuclei had migrated from the lumenal surface toward the basal region of the neuroepithelium (Fig. 1, Fig. S1, and Videos 1–3). As the apical-to-basal migration of NE cell nuclei is known to occur in G1 (Hollyday, 2001), this observation implies that the midbody is not necessarily released shortly after completion of mitosis but can be released when the daughter cell has progressed well into G1. Similarly, abscission may occur after the NE daughter cells have entered G1, as we observed aged apical midbodies (i.e., whose central region resembled P2 particles) that were still connected to daughter cells whose nuclei were already in an abventricular position (not depicted) and that had reformed a primary cilium (Fig. 3 E and Fig. S4 B).

The midbody as a source of extracellular membrane particles

The fate of the apical midbody of NE cells apparently is more complex than just to be released as a whole. We observed membrane buds of various sizes emerging from both cell-attached midbodies and midbody remnants detached from the cells (Figs. 3 and 4). Prom1 was concentrated on these buds (Fig. 4). The larger of the membrane vesicles arising from these buds may well correspond to those P2 prom1 particles that lack tubulin and anillin (Figs. 2 and 5) and thus do not appear to constitute complete midbodies (Fig. 8 B, b). The smaller of these buds may give rise to the P4 prom1 particles observed in the neural tube fluid and thus may constitute a second source of the latter particles in addition to microvilli (Marzesco et al., 2005; Fig. 8 B, a and b). The membrane vesicle budding from the detached midbodies probably corresponds to the previously observed midbody "deterioration" (Mullins and Biesele, 1977).

Importantly, given that plasma membrane protrusions showing prom1 clustering are known to contain specific membrane microdomains (Röper et al., 2000), our observations imply that the apical midbody of NE cells is a specific donor structure for extracellular membrane traffic, both while being cell attached and after its detachment.

Prom1 on primary cilia—an additional source of extracellular membrane vesicles?

The present study adds the primary cilium to the list of plasma membrane protrusions in which prom1 is concentrated. Interestingly, although the protrusions previously reported to bear prom1 (e.g., microvilli, lamellipodia, and filopodia; Weigmann et al., 1997; Corbeil et al., 2001; Fargeas et al., 2006) are actin based, the two types of structures found here to carry prom1, the midbody and the primary cilium, are microtubule based. Although the prom1-labeled apical midbodies account for the prom1-bearing pleiomorphic protuberances described previously (Marzesco et al., 2005), the presence of prom1 on primary cilia has not been noticed so far. In particular, two of our observations in this regard deserve comment. First, the finding that most (if not all) of the primary cilia of mouse NE cells at E10.5–13.5, i.e., at the onset of neurogenesis and thereafter, contained prom1 (Fig. 7, B–I), whereas at an earlier stage (E8.5), prom1 was barely detectable on primary cilia (Fig. 7 A), raises the possibility that the presence of prom1 on cilia is linked to the state of differentiation of these neural progenitor cells. The appearance of prom1 on cilia with the onset of neurogenesis is also consistent with the time course of appearance of P4 particles in the neural tube fluid (Marzesco et al., 2005).

Second, the distribution of prom1 on primary cilia suggests that small membrane vesicles bud from their tips. In a preliminary report, Huang et al. (Huang, K., Diener, D.R., Karki, R., Pedersen, L.B., Geimer, S., and Rosenbaum, J.L. 2005. American Society for Cell Biology Annual Meeting. Abstr. 1513), independently reached a similar conclusion for the cilia/flagella of *Chlamydomonas reinhardtii*, consistent with earlier observations in this organism by others (McLean et al., 1974; Bergman et al., 1975; Snell, 1976; Goodenough and Jurivich, 1978). If the small, P4 prom1 particles known to exist in the neural tube fluid (Marzesco et al., 2005) indeed originate, at least in part, from the primary cilia of NE cells (Fig. 8 B, c), this would raise the possibility that these organelles not only exhibit a signal-receiving function for their cells (Pazour and Witman, 2003; Hildebrandt and Otto, 2005; Pan et al., 2005; Hirokawa et al., 2006; Scholey and Anderson, 2006), but perhaps also a signal-sending function toward other cells. In addition, membrane budding from primary cilia may be part of the mechanism controlling their length, which varies between NE cells at different stages of development and at specific phases of the cell cycle (Fig. 7, A–H; Sorokin, 1968; Cohen et al., 1988).

The prom1 membrane microdomain as a link between primary cilium and midbody

It is interesting to note that primary cilia, which exist through interphase but not M phase (Hinds and Ruffett, 1971; Rieder et al., 1979; Cohen et al., 1988; Pan et al., 2005), and midbodies, whose existence is linked to M phase, share numerous components, including microtubule arrays and associated motor proteins, as well as specific protein kinases (Mullins and McIntosh, 1982; Gromley et al., 2003; Pan et al., 2004, 2005; Skop et al., 2004). The presence of the somatic stem cell membrane marker prom1 and the formation of prom1-bearing membrane buds on both primary cilia and apical midbodies of NE cells provide further support for a relationship between these two organelles. Processes in which these organelles may cooperate include (1) via their ability to release membrane particles, the reduction in the apical surface of NE cells that occurs during development and with the switch to neurogenesis (Kosodo et al., 2004; Marzesco et al., 2005) and (2) extrapolating from the role of primary cilia in polycystic kidney disease (Hildebrandt and Otto, 2005; Quarmby and Parker, 2005) the regulation of NE cell cycle progression.

Prom1, midbodies, and symmetric versus asymmetric division of NE cells

Our group previously showed that cleavages occurring approximately perpendicular to the ventricular surface of NE cells can be either symmetric or asymmetric, depending on whether the apical membrane is bisected or bypassed, respectively, by the cleavage furrow (Kosodo et al., 2004). According to this concept, only cleavages bisecting the apical membrane will, at the end of cytokinesis, form apical midbodies that contain prom1 on their surface (i.e., midbodies emerging apical to the adherens junction belt and constituting a cytoplasmic bridge connecting the apical surfaces of the two daughter cells [Fig. 8 A]). In contrast, cleavages bypassing the apical membrane would be expected to form midbodies at the apical-most end of the lateral membrane (including junctional complexes) that lack the apical membrane protein prom1. Our observations regarding apical (Fig. 6, A–E, E′, K–O, and O′) versus subapical (Fig. 6, F–J, J′, P–T, and T′) anillin clusters are consistent with this concept. Importantly, these imply that the midbody-derived prom1 particles in the lumen of the neural tube predominantly originate from NE cells undergoing symmetric, proliferative rather than asymmetric, neurogenic divisions. The accumulation in the neural tube fluid of the P2 prom1 particles before the onset of neurogenesis and their decline thereafter (Marzesco et al., 2005) is fully consistent with this notion.

There is an additional, major implication regarding the release of the lumenal prom1 particles from apical midbodies of NE cells. In HeLa cells, the midbody ring is inherited asymmetrically by one of the daughter cells and persists through interphase (Mishima et al., 2002; Gromley et al., 2005). Our observations imply that neural progenitor cells, in contrast to HeLa cells, prevent such asymmetry by releasing their apical midbody.

Significance of the prom1-bearing membrane and midbody release from neural progenitors

Why do NE cells, the primary progenitor cells of the mammalian central nervous system, cluster prom1, a somatic stem cell marker (Weigmann et al., 1997; Yin et al., 1997; Corbeil et al., 2001; Lee et al., 2005; Fargeas et al., 2006) and defining

constituent of a specific cholesterol-based membrane microdomain (Röper et al., 2000), at the midbody and release these membrane domains from, or together with, the midbody into the extracellular space? We previously discussed two possible roles of the release of prom1 particles from NE cells (which are not mutually exclusive): (1) disposal of a stem cell membrane microdomain and (2) intercellular signaling (Marzesco et al., 2005). In this regard, the present findings that the midbody of these neural progenitors is discharged into the neural tube lumen and is the source of the extracellular prom1 particles are particularly intriguing. In terms of disposal, the removal of the prom1-bearing membrane from the cell concomitant with the midbody would link the former precisely to the terminal step of the cell cycle, thereby ensuring the persistence of this membrane throughout, but not beyond, a given cell cycle. In terms of signaling, the release, by a given NE cell, of its apical midbody into the extracellular space could provide quantal information to the surrounding tissue about the history of division of that NE cell, i.e., that it underwent a symmetric, proliferative division. This may be important for controlling tissue growth. It will therefore be interesting to compare the fate of the midbody, including its specific membrane domains, between physiologically dividing and cancer cells.

Materials and methods

Prom1-GFP and GFP-anillin fusion constructs

An in-frame mouse prom1-GFP fusion construct was generated using standard cloning techniques (Roeper, K. 1997. Transport and sorting of prominin in Madin–Darby canine kidney cells. Diploma thesis. Free University of Berlin, Berlin, Germany. 86 pp.). The final fusion protein encoded full-length prom1 lacking its stop codon, followed by two linker amino acids (G and P) and GFP (containing the S65T exchange for enhancement of fluorescence). Expression of the prom1-GFP fusion protein in MDCK cells under the control of a constitutive promoter (CMV) followed by immunoblot, immunofluorescence, and cell surface biotinylation analyses revealed correct membrane topology; normal intracellular transport, glycosylation, and processing; and cell surface delivery selectively to the apical domain. The prom1-GFP fusion construct was inserted into the pCAGGS expression vector.

A fusion construct of GFP with the N terminus of mouse anillin$_{32\text{-}1121}$ (provided by Y. Kosodo, RIKEN, Kobe, Japan) was generated using standard cloning techniques. The GFP-anillin fusion construct was inserted into the pCAGGS expression vector. mRFP (Campbell et al., 2002) was also inserted into the pCAGGS expression vector to monitor the transfection of the chick spinal cord.

In ovo electroporation and live imaging

Chicken eggs (obtained from Lohmann Tierzucht GmbH) were incubated for 2 d in a humidified incubator at 38°C. At HH10–11, mouse prom1-GFP, GFP-anillin, and mRFP cDNAs (1–2 μg/μl), all driven by the cag promoter (CMV enhancer coupled to β-actin promoter; Niwa et al., 1991), were injected (<0.1 μl) into the lumen of the chick spinal cord and electroporated unidirectionally using a BTX electroporator by applying five pulses of 25 V for 30 ms each (Muramatsu et al., 1997; Momose et al., 1999).

After electroporation, eggs were incubated for 20–24 h, and spinal cord slice cultures were prepared and subjected to time-lapse fluorescence microscopy as described previously (Haubensak et al., 2004), with the following modifications. Transfected spinal cord regions were dissected and sliced manually with a razor blade (~400-μm-thick transverse slices). Slices were embedded in collagen (Cellmatrix type I-A; Nitta Gelatin, Inc.), which was diluted to 1–1.2 mg/ml in DME/F12 (Invitrogen), 26 mM $NaHCO_3$, 20 mM Hepes, and 5 mM NaOH; incubated for 20 min at 37°C to jellify; and covered with DME containing 100 U/ml penicillin/streptomycin, 10% chicken serum, and 5% fetal calf serum in a POC chamber at 37°C for imaging. Slices were imaged using an inverted confocal microscope (model IX81 [Olympus]; objective PlanApo 60× oil; NA 1.4) and imaging system (FluoView 1000; Olympus). Acquisition of fluorescent and differential interference contrast (DIC) images was performed simultaneously at a depth of 40–80 μm in the slice. Approximately 10 optical sections were collected in the z axis, with 1–1.2-μm steps. Imaging was performed either for 0.5–1.5 h, with the slice being scanned every 35–120 s, or for almost 7 h, with the slice being scanned every 5 min. Images were analyzed with Imaris software (Bitplane), level and gamma value were adjusted, and images were assembled with Photoshop and Image Ready (Adobe).

Immunohistological analyses

Mouse embryos of NMRI wild type, the *Tis21*$^{GFP/+}$ knockin line (C57BL6 background; Haubensak et al., 2004), and the prom1 knockout line (generated in the laboratory of P. Carmeliet, University of Leuven, Leuven, Belgium), and electroporated chick embryos were fixed in 4% paraformaldehyde and cryosectioned. For immunostaining, sections (14–18 μm) were incubated with rat mAb 13A4 against mouse prom1 (1.2 μg/ml; Weigmann et al., 1997), affinity-purified rabbit anti-megalin antibody (1 μg/ml; obtained from S. Argraves, Medical University of South Carolina, Charleston, SC; Drake et al., 2004), affinity-purified rabbit anti-anillin antibody (1:400; obtained from C. Field, Harvard Medical School, Boston, MA; Oegema et al., 2000), mouse mAb against α-tubulin (1:400, Sigma-Aldrich), and mouse mAb recognizing pan-cadherin (1:200; Sigma-Aldrich), followed by Cy3- and Cy5-conjugated secondary antibodies (1:1,000; Jackson ImmunoResearch Laboratories). Nuclei were stained with DAPI (125 ng/ml; Sigma-Aldrich). Images were acquired either on a conventional fluorescent microscope (model BX61 [Olympus]; camera and acquisition device obtained from Diagnostic Instruments, Inc., and ViSytron Systems with IPLab software) or with an inverted microscope (Axiovert 200; Carl Zeiss MicroImaging, Inc.) and laser-scanning confocal imaging system (LSM 510 [Carl Zeiss MicroImaging, Inc.]; PlanApo 63× oil; DIC objective, NA 1.4) used in conjunction with LSM 510 AIM acquisition software (Carl Zeiss MicroImaging, Inc.) using 1-μm z steps (pinhole at 1 area unit for prom1, cadherin, and anillin), and processed with Photoshop.

For anillin versus prom1 localization by double immunofluorescence, only mitotic NE cells at the ventricular surface were analyzed, in which anillin was clustered at the apical surface, i.e., cells in late telophase. We first analyzed whether such apically clustered anillin was colocalized with (symmetric division) or distinct from (asymmetric division) prom1. This analysis was performed without knowledge by the investigator of *Tis21*-GFP expression, which was determined subsequently.

For anillin versus cadherin localization by double immunofluorescence, only mitotic NE cells at the ventricular surface were analyzed, in which anillin was either clustered at the apical surface, i.e., cells in late telophase, or at least associated with the contractile ring of cells in anaphase or telophase. Following previously described methods (Kosodo et al., 2004), the orientation of the cleavage plane was first deduced from the orientation of the sister chromatids and then corroborated by the orientation of the contractile ring as revealed by anillin immunostaining (in the case of incomplete [0–80%] ingression of the cleavage furrow) or the orientation of the cleavage furrow as revealed by cadherin immunostaining (in the case of complete [90–100%] ingression of the cleavage furrow). We then determined whether cleavage would be predicted to bisect (symmetric division) or bypass (asymmetric division) the apical membrane, revealed by cadherin immunostaining as cadherin "hole" (Kosodo et al., 2004). In the case of complete ingression of the cleavage furrow, the localization of the midbody (revealed by anillin immunostaining) relative to the cadherin hole served as additional, decisive criterion. Symmetric versus asymmetric division was determined without knowledge by the investigator of *Tis21*-GFP expression, which was scored last as either weak or strong. Only mitotic NE cells in which symmetric versus asymmetric division could be determined unambiguously and that received the same scoring independently by two investigators were considered, and only cells showing 90–100% complete ingression of the cleavage furrow were eventually included in the quantification. 3D reconstruction of anillin versus prom1 or cadherin immunofluorescence and DAPI staining was performed from six to eight optical sections after applying a Gaussian filter, using Imaris 4.1.1 software, specifically the Iso Surface function with appropriate threshold settings.

Immunoblotting

Neural tube fluid of wild-type E11.5 NMRI mouse embryo was collected and fractionated by differential centrifugation, and fractions were analyzed by immunoblotting using mouse mAb against α-tubulin (1:4,000; Sigma-Aldrich) as described previously (Marzesco et al., 2005).

Conventional transmission EM
Mouse embryos were fixed for 1–2 h in 4% paraformaldehyde and overnight in 2% glutaraldehyde, both in phosphate buffer. Defined regions of the embryonic brain were cut and processed for EM. The tissue was postfixed with 1% osmium tetroxide and dehydrated through a graded series of ethanol at room temperature (15–30 min for each step) before infiltration with EmBed resin (Science Services) and polymerization at 60°C for 2 d. Ultrathin sections (70 nm) were cut on a UCT microtome (Leica Microsystems) and viewed in an electron microscope (Morgagni; FEI Company). Micrographs were taken with a charge-coupled device camera (MegaviewII; Soft Imaging System) and AnalySis software (Soft Imaging System) or with plate negatives (SO163; Kodak), which were scanned on a flatbed scanner (PowerLook 1100; UMAX) with transmitted light and processed with Photoshop.

Postembedding immunogold transmission EM
Samples of mouse embryonic brain were processed for Tokuyashu cryosectioning and subsequent single or double immunogold labeling as previously described (Marzesco et al., 2005). The following antibodies were used: 25–50 μg/ml mAb 13A4 followed by rabbit antiserum to rat IgG (Cappel) and protein A/5 nm gold (Utrecht University); rabbit antibodies against anillin and megalin (see Immunohistochemistry) followed in either case by protein A/10 nm gold; and mouse IgG1 against α-tubulin (1:600; Sigma-Aldrich) or mouse IgG2b against acetylated tubulin (1:100; clone 6-11B-1; Sigma-Aldrich) followed by a secondary goat antibody anti-mouse IgG/M coupled to 12 nm gold (Dianova).

Immunogold transmission EM of subcellular fractions
The P2 pellet, isolated by differential centrifugation of neural tube fluid isolated from 23 E10.5 mice (Marzesco et al., 2005), was resuspended in 4% paraformaldehyde in phosphate buffer and adsorbed to 400 mesh formvar/carbon-coated grids. The samples were processed through immunogold labeling and negative contrasting as described previously (Marzesco et al., 2005).

Preembedding immunogold transmission EM
E8.5–12.5 mice were fixed for at least 24 h in 4% paraformaldehyde in phosphate buffer and stored in fixative until use. E8.5 embryos were manually cut into small pieces, whereas older embryos were embedded in 3% low-melting agarose and 200-μm-thick vibratome sections (VT1000S; Leica Microsystems) were prepared. In the case of the vibratome sections, the surrounding agarose was removed before postfixation in 4% paraformaldehyde in phosphate buffer. Tissue pieces and vibratome sections were blocked with 0.5% BSA and 0.2% gelatine in PBS before incubation with 1 μg/ml rat mAb 13A4 for 2 h at room temperature. After washing in blocking buffer, samples were postfixed in 4% paraformaldehyde, blocked, and incubated with rabbit antiserum against rat IgG (1:1,000) followed by protein A/10 nm gold. Samples were washed with PBS and postfixed with 1% glutaraldehyde in phosphate buffer for 15 min at room temperature. Samples were then processed for plastic embedding as described above (see Conventional transmission EM). Contrast settings of scanned micrographs as whole (see Conventional transmission EM) were increased with Photoshop.

Immunogold-labeling scanning EM
Prom1 immunogold labeling for scanning EM was performed with E10.5 embryos as described (see Preembedding immunogold transmission EM), except that the brain ventricles were opened manually by a sagittal cut, and a goat anti-rabbit antibody coupled to 18 nm gold (Dianova) was used instead of protein A. Glutaraldehyde-postfixed samples were processed for detection of the backscattered electrons by scanning EM as described previously (Steegmaier et al., 1997).

Online supplemental material
The formation of GFP-anillin–containing particles at the apical surface of NE cells at the end of cytokinesis is shown in Fig. S1 and Video 3. A midbody and electron-dense particles containing prom1 in the lumen of the chick spinal cord are displayed in Fig. S2. Fig. S3 and the corresponding text describe that the megalin-containing apical membrane subdomain does not overlap with the prom1-containing membrane subdomain. Fig. S4 provides the complete series of micrographs from which Fig. 3 (A and E–H) was selected. Videos 1 and 2 show the release of prom1-GFP–bearing particles from the apical surface of NE cells. Videos 4–7 provide an animation of the 3D reconstructions shown in Fig. 6 (E′, J′, O′, and T′). Online supplemental material is available at http://www.jcb.org/cgi/content/full/jcb.200608137/DC1.

We are indebted to Dr. C. Field for providing us with affinity-purified anillin antibody; we thank Dr. K. Röper for generating and characterizing the mouse prom1-GFP fusion; Dr. Y. Kosodo for providing the GFP-anillin construct, K. Langenfeld for excellent technical assistance; the Biomedical Services (Y. Helppi) and the Light Microscopy Facility (J. Peychl) of MPI-CBG for expert support; Dr. P. Carmeliet and colleagues for kindly providing the prom1 knockout mouse line; Dr. S. Argraves for megalin antibody; Dr. H. Schwarz and J. Berger for help with immunogold scanning EM; Drs. J. Howard and A. Hyman for helpful discussion; and Dr. S. Eaton for her insightful comments on the manuscript.

V. Dubreuil was supported by an EMBO long-term fellowship; D. Corbeil by grants from the Deutsche Forschungsgemeinschaft (SFB/TR13-04 B1 and SFB 655 A13) and Sächsisches Ministerium für Wissenschaft und Kunst, Europäischer Fond für Regionale Entwicklung (4212/05-16); and W.B. Huttner by grants from the Deutsche Forschungsgemeinschaft (SPP 1109, Hu275/7-3; SPP 1111, Hu275/8-3; SFB/TR13-04, B1; and SFB 655, A2) and the Federal Ministry of Education and Research (NGFN, SMP RNAi, 01GR0402, and PRI-S08T05).

Submitted: 22 August 2006
Accepted: 6 January 2007

References

Aaku-Saraste, E., B. Oback, A. Hellwig, and W.B. Huttner. 1997. Neuroepithelial cells downregulate their plasma membrane polarity prior to neural tube closure and neurogenesis. *Mech. Dev.* 69:71–81.

Allenspach, A.L., and L.E. Roth. 1967. Structural variations during mitosis in the chick embryo. *J. Cell Biol.* 33:179–196.

Bancroft, M., and R. Bellairs. 1975. Differentiation of the neural plate and neural tube in the young chick embryo. A study by scanning and transmission electron microscopy. *Anat. Embryol. (Berl.).* 147:309–335.

Beaudoin, A.R., and G. Grondin. 1991. Shedding of vesicular material from the cell surface of eukaryotic cells: different cellular phenomena. *Biochim. Biophys. Acta.* 1071:203–219.

Bellairs, R., and M. Bancroft. 1975. Midbodies and beaded threads. *Am. J. Anat.* 143:393–398.

Bergman, K., U.W. Goodenough, D.A. Goodenough, J. Jawitz, and H. Martin. 1975. Gametic differentiation in *Chlamydomonas reinhardtii*. II. Flagellar membranes and the agglutination reaction. *J. Cell Biol.* 67:606–622.

Buck, R.C., and J.M. Tidsale. 1962a. An electron microscopic study of the cleavage furrow in mammalian cells. *J. Cell Biol.* 13:117–125.

Buck, R.C., and J.M. Tisdale. 1962b. The fine structure of the mid-body of the rat erythroblast. *J. Cell Biol.* 13:109–115.

Campbell, R.E., O. Tour, A.E. Palmer, P.A. Steinbach, G.S. Baird, D.A. Zacharias, and R.Y. Tsien. 2002. A monomeric red fluorescent protein. *Proc. Natl. Acad. Sci. USA.* 99:7877–7882.

Chenn, A., and S.K. McConnell. 1995. Cleavage orientation and the asymmetric inheritance of Notch1 immunoreactivity in mammalian neurogenesis. *Cell.* 82:631–641.

Cohen, E., S. Binet, and V. Meininger. 1988. Ciliogenesis and centriole formation in the mouse embryonic nervous system. An ultrastructural analysis. *Biol. Cell.* 62:165–169.

Corbeil, D., K. Röper, C.A. Fargeas, A. Joester, and W.B. Huttner. 2001. Prominin: a story of cholesterol, plasma membrane protrusions and human pathology. *Traffic.* 2:82–91.

Drake, C.J., P.A. Fleming, A.C. Larue, J.L. Barth, M.R. Chintalapudi, and W.S. Argraves. 2004. Differential distribution of cubilin and megalin expression in the mouse embryo. *Anat. Rec. A Discov. Mol. Cell. Evol. Biol.* 277:163–170.

Fargeas, C.A., D. Corbeil, and W.B. Huttner. 2003. AC133 antigen, CD133, prominin-1, prominin-2, etc.: prominin family gene products in need of a rational nomenclature. *Stem Cells.* 21:506–508.

Fargeas, C.A., A.-V. Fonseca, W.B. Huttner, and D. Corbeil. 2006. Prominin-1 (CD133): from progenitor cells to human diseases. *Future Lipidology.* 1:213–225.

Field, C.M., and B.M. Alberts. 1995. Anillin, a contractile ring protein that cycles from the nucleus to the cell cortex. *J. Cell Biol.* 131:165–178.

Février, B., and G. Raposo. 2004. Exosomes: endosomal-derived vesicles shipping extracellular messages. *Curr. Opin. Cell Biol.* 16:415–421.

Glotzer, M. 2001. Animal cell cytokinesis. *Annu. Rev. Cell Dev. Biol.* 17:351–386.

Golsteyn, R.M., S.J. Schultz, J. Bartek, A. Ziemiecki, T. Ried, and E.A. Nigg. 1994. Cell cycle analysis and chromosomal localization of human

Plk1, a putative homologue of the mitotic kinases *Drosophila* polo and *Saccharomyces cerevisiae* Cdc5. *J. Cell Sci.* 107:1509–1517.

Goodenough, U.W., and D. Jurivich. 1978. Tipping and mating-structure activation induced in *Chlamydomonas* gametes by flagellar membrane antisera. *J. Cell Biol.* 79:680–693.

Gromley, A., A. Jurczyk, J. Sillibourne, E. Halilovic, M. Mogensen, I. Groisman, M. Blomberg, and S. Doxsey. 2003. A novel human protein of the maternal centriole is required for the final stages of cytokinesis and entry into S phase. *J. Cell Biol.* 161:535–545.

Gromley, A., C. Yeaman, J. Rosa, S. Redick, C.T. Chen, S. Mirabelle, M. Guha, J. Sillibourne, and S.J. Doxsey. 2005. Centriolin anchoring of exocyst and SNARE complexes at the midbody is required for secretory-vesicle-mediated abscission. *Cell.* 123:75–87.

Götz, M., and W.B. Huttner. 2005. The cell biology of neurogenesis. *Nat. Rev. Mol. Cell Biol.* 6:777–788.

Haubensak, W., A. Attardo, W. Denk, and W.B. Huttner. 2004. Neurons arise in the basal neuroepithelium of the early mammalian telencephalon: a major site of neurogenesis. *Proc. Natl. Acad. Sci. USA.* 101:3196–3201.

Hildebrandt, F., and E. Otto. 2005. Cilia and centrosomes: a unifying pathogenic concept for cystic kidney disease? *Nat. Rev. Genet.* 6:928–940.

Hinds, J.W., and T.L. Ruffett. 1971. Cell proliferation in the neural tube: an electron microscopic and Golgi analysis in the mouse cerebral vesicle. *Z. Zellforsch. Mikrosk. Anat.* 115:226–264.

Hirokawa, N., Y. Tanaka, Y. Okada, and S. Takeda. 2006. Nodal flow and the generation of left-right asymmetry. *Cell.* 125:33–45.

Hobbs, D.G. 1980. The origin and distribution of membrane-bound vesicles associated with the brush border of chick intestinal mucosa. *J. Anat.* 131:635–642.

Hollyday, M. 2001. Neurogenesis in the vertebrate neural tube. *Int. J. Dev. Neurosci.* 19:161–173.

Huangfu, D., and K.V. Anderson. 2005. Cilia and Hedgehog responsiveness in the mouse. *Proc. Natl. Acad. Sci. USA.* 102:11325–11330.

Jones, O.P. 1969. Elimination of midbodies from mitotic erythroblasts and their contribution to fetal blood plasma. *J. Natl. Cancer Inst.* 42:753–759.

Kosodo, Y., K. Röper, W. Haubensak, A.-M. Marzesco, D. Corbeil, and W.B. Huttner. 2004. Asymmetric distribution of the apical plasma membrane during neurogenic divisions of mammalian neuroepithelial cells. *EMBO J.* 23:2314–2324.

Krull, C.E. 2004. A primer on using in ovo electroporation to analyze gene function. *Dev. Dyn.* 229:433–439.

Lee, A., J.D. Kessler, T.A. Read, C. Kaiser, D. Corbeil, W.B. Huttner, J.E. Johnson, and R.J. Wechsler-Reya. 2005. Isolation of neural stem cells from the postnatal cerebellum. *Nat. Neurosci.* 8:723–729.

Low, S.H., X. Li, M. Miura, N. Kudo, B. Quinones, and T. Weimbs. 2003. Syntaxin 2 and endobrevin are required for the terminal step of cytokinesis in mammalian cells. *Dev. Cell.* 4:753–759.

Marzesco, A.M., P. Janich, M. Wilsch-Brauninger, V. Dubreuil, K. Langenfeld, D. Corbeil, and W.B. Huttner. 2005. Release of extracellular membrane particles carrying the stem cell marker prominin-1 (CD133) from neural progenitors and other epithelial cells. *J. Cell Sci.* 118:2849–2858.

Matheson, J., X. Yu, A.B. Fielding, and G.W. Gould. 2005. Membrane traffic in cytokinesis. *Biochem. Soc. Trans.* 33:1290–1294.

McLean, R., C.J. Laurendi, and R.M. Brown Jr. 1974. The relationship of gamone to the mating reaction in *Chlamydomonas moewusii*. *Proc. Natl. Acad. Sci. USA.* 71:2610–2613.

Mishima, M., S. Kaitna, and M. Glotzer. 2002. Central spindle assembly and cytokinesis require a kinesin-like protein/RhoGAP complex with microtubule bundling activity. *Dev. Cell.* 2:41–54.

Momose, T., A. Tonegawa, J. Takeuchi, H. Ogawa, K. Umesono, and K. Yasuda. 1999. Efficient targeting of gene expression in chick embryos by microelectroporation. *Dev. Growth Differ.* 41:335–344.

Mullins, J.M., and J.J. Biesele. 1977. Terminal phase of cytokinesis in D-98s cells. *J. Cell Biol.* 73:672–684.

Mullins, J.M., and J.R. McIntosh. 1982. Isolation and initial characterization of the mammalian midbody. *J. Cell Biol.* 94:654–661.

Muramatsu, T., Y. Mizutani, Y. Ohmori, and J. Okumura. 1997. Comparison of three nonviral transfection methods for foreign gene expression in early chicken embryos in ovo. *Biochem. Biophys. Res. Commun.* 230:376–380.

Nagele, R.G., and H.Y. Lee. 1979. Ultrastructural changes in cells associated with interkinetic nuclear migration in the developing chick neuroepithelium. *J. Exp. Zool.* 210:89–106.

Niwa, H., K. Yamamura, and J. Miyazaki. 1991. Efficient selection for high-expression transfectants with a novel eukaryotic vector. *Gene.* 108:193–199.

Oegema, K., M.S. Savoian, T.J. Mitchison, and C.M. Field. 2000. Functional analysis of a human homologue of the *Drosophila* actin binding protein anillin suggests a role in cytokinesis. *J. Cell Biol.* 150:539–552.

Otegui, M.S., K.J. Verbrugghe, and A.R. Skop. 2005. Midbodies and phragmoplasts: analogous structures involved in cytokinesis. *Trends Cell Biol.* 15:404–413.

Pan, J., Q. Wang, and W.J. Snell. 2004. An aurora kinase is essential for flagellar disassembly in *Chlamydomonas*. *Dev. Cell.* 6:445–451.

Pan, J., Q. Wang, and W.J. Snell. 2005. Cilium-generated signaling and cilia-related disorders. *Lab. Invest.* 85:452–463.

Pazour, G.J., and G.B. Witman. 2003. The vertebrate primary cilium is a sensory organelle. *Curr. Opin. Cell Biol.* 15:105–110.

Praetorius, H.A., and K.R. Spring. 2005. A physiological view of the primary cilium. *Annu. Rev. Physiol.* 67:515–529.

Quarmby, L.M., and J.D. Parker. 2005. Cilia and the cell cycle? *J. Cell Biol.* 169:707–710.

Rieder, C.L., C.G. Jensen, and L.C. Jensen. 1979. The resorption of primary cilia during mitosis in a vertebrate (PtK1) cell line. *J. Ultrastruct. Res.* 68:173–185.

Robbins, E., and N.K. Gonatas. 1964. The ultrastructure of a mammalian cell during the mitotic cycle. *J. Cell Biol.* 21:429–463.

Rosenbaum, J.L., and G.B. Witman. 2002. Intraflagellar transport. *Nat. Rev. Mol. Cell Biol.* 3:813–825.

Röper, K., D. Corbeil, and W.B. Huttner. 2000. Retention of prominin in microvilli reveals distinct cholesterol-based lipid microdomains in the apical plasma membrane. *Nat. Cell Biol.* 2:582–592.

Scholey, J.M., and K.V. Anderson. 2006. Intraflagellar transport and cilium-based signaling. *Cell.* 125:439–442.

Schweitzer, J.K., and C. D'Souza-Schorey. 2004. Finishing the job: cytoskeletal and membrane events bring cytokinesis to an end. *Exp. Cell Res.* 295:1–8.

Skop, A.R., H. Liu, J. Yates III, B.J. Meyer, and R. Heald. 2004. Dissection of the mammalian midbody proteome reveals conserved cytokinesis mechanisms. *Science.* 305:61–66.

Snell, W.J. 1976. Mating in *Chlamydomonas*: a system for the study of specific cell adhesion. I. Ultrastructural and electrophoretic analyses of flagellar surface components involved in adhesion. *J. Cell Biol.* 68:48–69.

Snell, W.J., J. Pan, and Q. Wang. 2004. Cilia and flagella revealed: from flagellar assembly in *Chlamydomonas* to human obesity disorders. *Cell.* 117:693–697.

Sorokin, S.P. 1968. Reconstructions of centriole formation and ciliogenesis in mammalian lungs. *J. Cell Sci.* 3:207–230.

Steegmaier, M., E. Borges, J. Berger, H. Schwarz, and D. Vestweber. 1997. The E-selectin-ligand ESL-1 is located in the Golgi as well as on microvilli on the cell surface. *J. Cell Sci.* 110:687–694.

Stoorvogel, W., M.J. Kleijmeer, H.J. Geuze, and G. Raposo. 2002. The biogenesis and functions of exosomes. *Traffic.* 3:321–330.

Tanaka, Y., Y. Okada, and N. Hirokawa. 2005. FGF-induced vesicular release of Sonic hedgehog and retinoic acid in leftward nodal flow is critical for left-right determination. *Nature.* 435:172–177.

Théry, C., L. Zitvogel, and S. Amigorena. 2002. Exosomes: composition, biogenesis and function. *Nat. Rev. Immunol.* 2:569–579.

Weigmann, A., D. Corbeil, A. Hellwig, and W.B. Huttner. 1997. Prominin, a novel microvilli-specific polytopic membrane protein of the apical surface of epithelial cells, is targeted to plasmalemmal protrusions of non-epithelial cells. *Proc. Natl. Acad. Sci. USA.* 94:12425–12430.

Yin, A.H., S. Miraglia, E.D. Zanjani, G. Almeida-Porada, M. Ogawa, A.G. Leary, J. Olweus, J. Kearney, and D.W. Buck. 1997. AC133, a novel marker for human hematopoietic stem and progenitor cells. *Blood.* 90:5002–5012.